Protist, Vol. 170, 82–103, February 2019
http://www.elsevier.de/protis
Published online date 21 December 2018

Protist

ORIGINAL PAPER

Tuberlatum coatsi gen. n., sp. n. (Alveolata, Perkinsozoa), a New Parasitoid with Short Germ Tubes Infecting Marine Dinoflagellates

Boo Seong Jeon, and Myung Gil Park[1]

LOHABE, Department of Oceanography, Chonnam National University, Gwangju 61186, Republic of Korea

Submitted October 16, 2018; Accepted December 15, 2018
Monitoring Editor: Laure Guillou

Perkinsozoa is an exclusively parasitic group within the alveolates and infections have been reported from various organisms, including marine shellfish, marine dinoflagellates, freshwater cryptophytes, and tadpoles. Despite its high abundance and great genetic diversity revealed by recent environmental rDNA sequencing studies, Perkinsozoa biodiversity remains poorly understood. During the intensive samplings in Korean coastal waters during June 2017, a new parasitoid of dinoflagellates was detected and was successfully established in culture. The new parasitoid was most characterized by the presence of two to four dome-shaped, short germ tubes in the sporangium. The opened germ tubes were biconvex lens-shaped in the top view and were characterized by numerous wrinkles around their openings. Phylogenetic analyses based on the concatenated SSU and LSU rDNA sequences revealed that the new parasitoid was included in the family Parviluciferaceae, in which all members were comprised of two separate clades, one containing *Parvilucifera* species (*P. infectans*, *P. corolla*, and *P. rostrata*), and the other containing *Dinovorax pyriformis*, *Snorkelia* spp., and the new parasitoid from this study. Based on morphological, ultrastructural, and molecular data, we propose to erect a new genus and species, *Tuberlatum coatsi* gen. n., sp. n., from the new parasitoid found in this study. Further, we examined and discussed the validity of some diagnostic characteristics reported for parasitoids in the family Parviluciferaceae at both the genus and species levels.

Key words: Life-cycle; parasite; parasitism; phylogeny; protist; ultrastructure.

Introduction

Perkinsozoa is a parasitic group within the alveolates that occupies the earliest branching phylogenetic position within the Dinozoa (Bachvaroff et al. 2014). Several recent studies based on environmental rDNA sequencing revealed that Perkinsozoa is highly abundant and widespread in aquatic environments, from freshwater to marine, as well as in sediments (Bråte et al. 2010; Chambouvet et al. 2014; Lepère et al. 2008; Mangot et al. 2011). Perkinsozoa infections have been reported from a variety of organisms, including marine shellfishes such as oysters and clams (Levine, 1978), marine dinoflagellates (Norén et al.

[1]Corresponding author; fax +82-62-530-3468
e-mail mpark@chonnam.ac.kr (M.G. Park).

https://doi.org/10.1016/j.protis.2018.12.003
1434-4610/

1999), freshwater cryptophytes (Brugerolle 2002), and tadpoles (Chambouvet et al. 2015). Despite its great genetic diversity, however, only three representative groups of Perkinsozoa have been thus far described morphologically and taxonomically: *Perkinsus* spp. Levine (Levine 1978), *Rastrimonas subtilis* (previously known as *Cryptophagus subtilis*) (Brugerolle 2002), and the members of the family Parviluciferaceae (Reñé et al. 2017a).

The Family Parviluciferaceae, which was erected by Reñé et al. (2017a), contains three genera: *Dinovorax*, *Snorkelia*, and *Parvilucifera*. These parasitoids use marine dinoflagellates as hosts and have a similar life-history consisting of three stages: free-living zoospores, trophocytes, and sporocytes. The free-living zoospores penetrate the cytoplasm of their host and consume host materials, developing into a trophont. At maturation, the trophont undergoes nuclear division, followed by cytokinesis, producing numerous zoospores. The mature zoospores escape from the sporangium to infect new hosts. Among Parviluciferaceae members, two genera *Dinovorax* and *Snorkelia* develop a relatively long (10 ~ 15 μm) germ tube (=discharge tube) at the sporocyte stage for the release of zoospores, whereas species belonging to the genus *Parvilucifera* do not develop any germ tube(s) and instead have several apertures for zoospore release (Figueroa et al. 2008; Leander and Hoppenrath 2008; Lepelletier et al. 2014; Norén et al. 1999; Reñé et al. 2017a,b).

During intensive sampling along the Korean coast in June 2017, a novel parasitoid belonging to Parviluciferaceae was detected and was successfully established in culture. Based on morphological, ultrastructural and molecular data, the parasitoid showed distinct morphological and genetic differences from the extant Parviluciferaceae members, which raised the need to erect a new genus for *Tuberlatum coatsi* gen. nov. et sp. nov.

Results

Life-cycle of *Tuberlatum coatsi* and the Morphology of its Developmental Stages

Infection occurred when a free-living zoospore penetrated the dinoflagellate host *A. catenella* strain Ac-LOHABE01, probably through the flagellar pore region, during which the host lost its swimming ability and sank to the bottom of the culture dish. It transformed into a spherical trophont while consuming the host cytoplasm, which was easily recognizable at 24 h after penetration by the presence of a round body in the cytoplasm of the host cell under light microscopy (Fig. 1A). Multiple infections were commonly observed in a single host cell (Fig. 1B). Up to 9 infections could simultaneously occur and develop in the same host cell when infecting the large dinoflagellate *Pyrophacus steinii* (pers. observ.). The trophont continued to grow and increase in size by consuming the host cytoplasm until it occupied most of the host cell (Fig. 1C, D). At the late trophocyte stage, 54 h after penetration, when host cytoplasm was almost completely consumed, the nucleus of the parasitoid was visible when stained with SYBR gold (Fig. 2B-F). At this stage, the cytoplasmic content of the parasitoid was located at the periphery, with the central area occupied by hyaline material (Fig. 2A). This stage was followed by the early sporocyte stage, during which schizogony resulted in the production of new nuclei arranged along the sporocyte periphery (Fig. 2G-L). At the early to middle sporocyte stage, dome-shaped, short (average ratio of 1:8 = the length of the germ tube relative to the diameter of the sporangium) and wide (8 ~ 15.4 μm in major axis) germ tubes (syn. discharge tube) began to develop (Figs 1E, F, G, 3A, B, C), and nuclear divisions continued, resulting in the observation of several smaller nuclei at the periphery (Fig. 2M-R). Up to 4 germ tubes in a single sporangium were sometimes observed (n = 10). During the late stage of infection, the sporangium was full of numerous new zoospores, which had small rounded nuclei (Fig. 2S-X), and the shape of the mature sporangium was slightly oval with a single infection but was highly variable with multiple infections (Fig. 1H, I). The surface of the sporangium was smooth and did not have any process (Fig. 3). When the zoospores were fully developed and ready to escape, they swam for 5 ~ 10 min within the sporangium and then escaped from the sporangium through the open germ tube(s) (Fig. 1J, K). It took approximately 15 ~ 20 min for most zoospores to escape from the sporangium. When zoospores were released, a round residual body frequently remained inside the sporangium (Fig. 1M). Under the growth conditions described above, it took 92 h from the penetration into *A. catenella* to the zoospore release. After the release of zoospores, the opened germ tubes looked like biconvex lens in shape in top view (approximately 7 ~ 9 μm in the major axis and 3 ~ 5 μm in the minor axis) and were characterized by numerous wrinkles around their openings (Figs 1L, 3D, E, F). The zoospores just released from the sporangium remained sluggish for a while at the bottom of the culture dish, and then they dispersed into

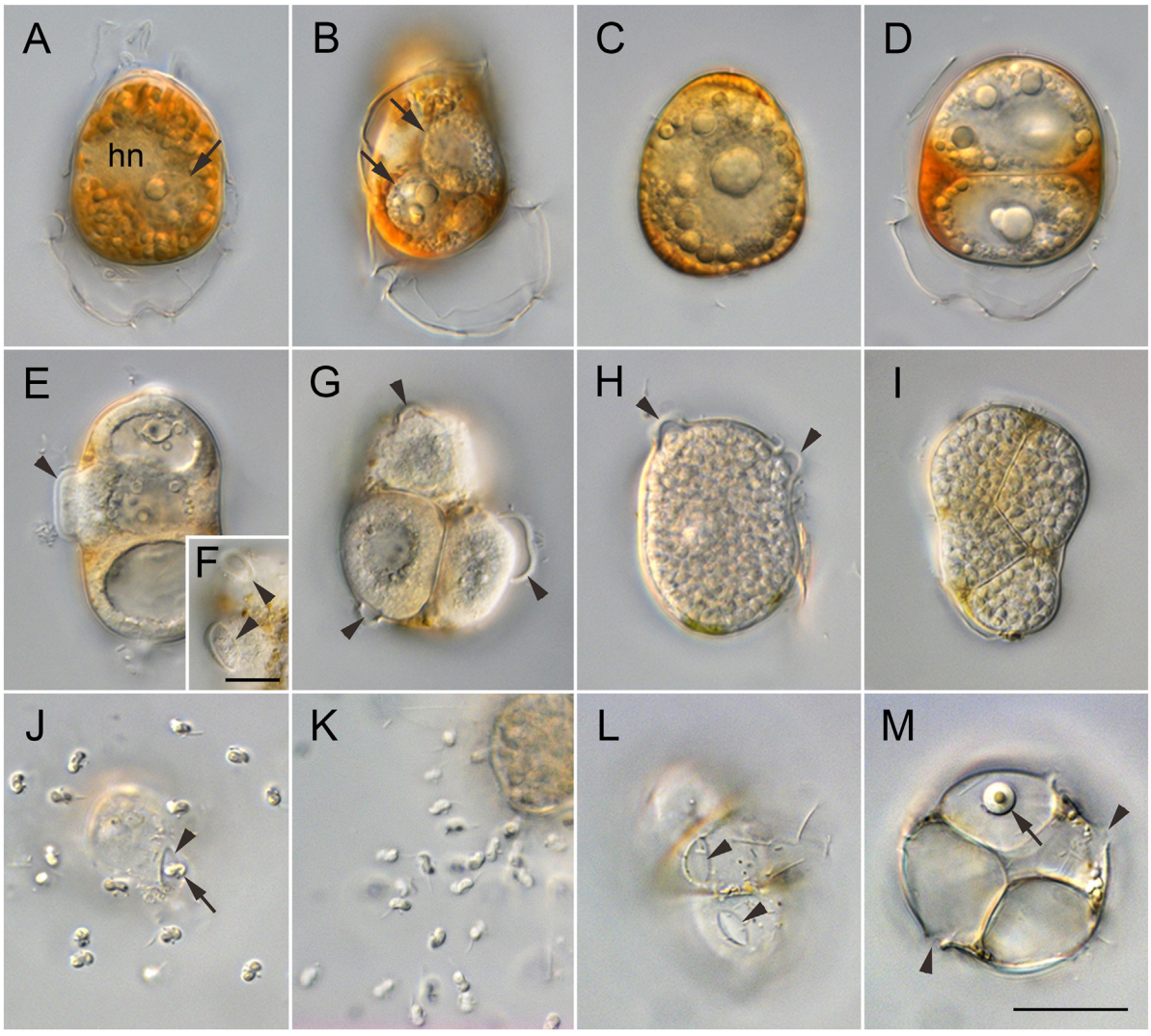

Figure 1. Differential interference contrast (DIC) images showing the life-cycle stages of *Tuberlatum coatsi* gen. nov. et sp. nov. in dinoflagellate host *Alexandrium catenella*. **A**. The early trophocyte (arrow) within host cytoplasm. Host nucleus (hn) is also visible. **B**. Two trophocytes (arrows) developed within a host cell. **C**. The late trophocyte almost consumed host cytoplasm. **D**. Two late trophocytes growing simultaneously within the host cell. **E**. The formation of the germ tube (arrowhead) from early to middle sporocytes. **F**. The germ tubes (arrowheads) with biconvex lens-shape in top view. **G**. Three middle to late sporocytes with germ tubes (arrowheads). **H**. The mature sporangium of *T. coatsi* with two germ tubes (arrowheads). **I**. The four fully developed mature sporangia. **J**. Zoospores (arrow) escaping from the opened germ tube (arrowhead). **K**. The sluggish zoospores just released from sporangium. **L**. The empty sporangia and biconvex lens-shaped opened germ tubes (arrowheads). **M**. The empty four sporangia, in which one retains a residual body (arrow). Germ tubes (arrowheads) are also visible. The scale bar in M is 20 μm and applies to all panels, except for F = 10 μm.

the water column (Supplementary Material Video S1). The number of zoospores produced per sporangium appeared to be dependent on sporangium biovolume. When single infection occurred in *A. catenella*, the mature sporangium had a diameter of 19 ~ 34 μm (corresponding to 3,500 ~ 20,000 μm^3 in volume) and contained 111 ± 7.5 zoospores per 10^3 μm^3 sporangium volume (mean ± SE, n = 6).

Ultrastructure of *Tuberlatum coatsi* Life-cycle Stages

In the early stage of infection, the immature trophont developed within the parasitophorous vacuole. Multiple infections in the same host cell were frequently observed (Fig. 4A). The trophont gradually grew, increasing in size while consum-

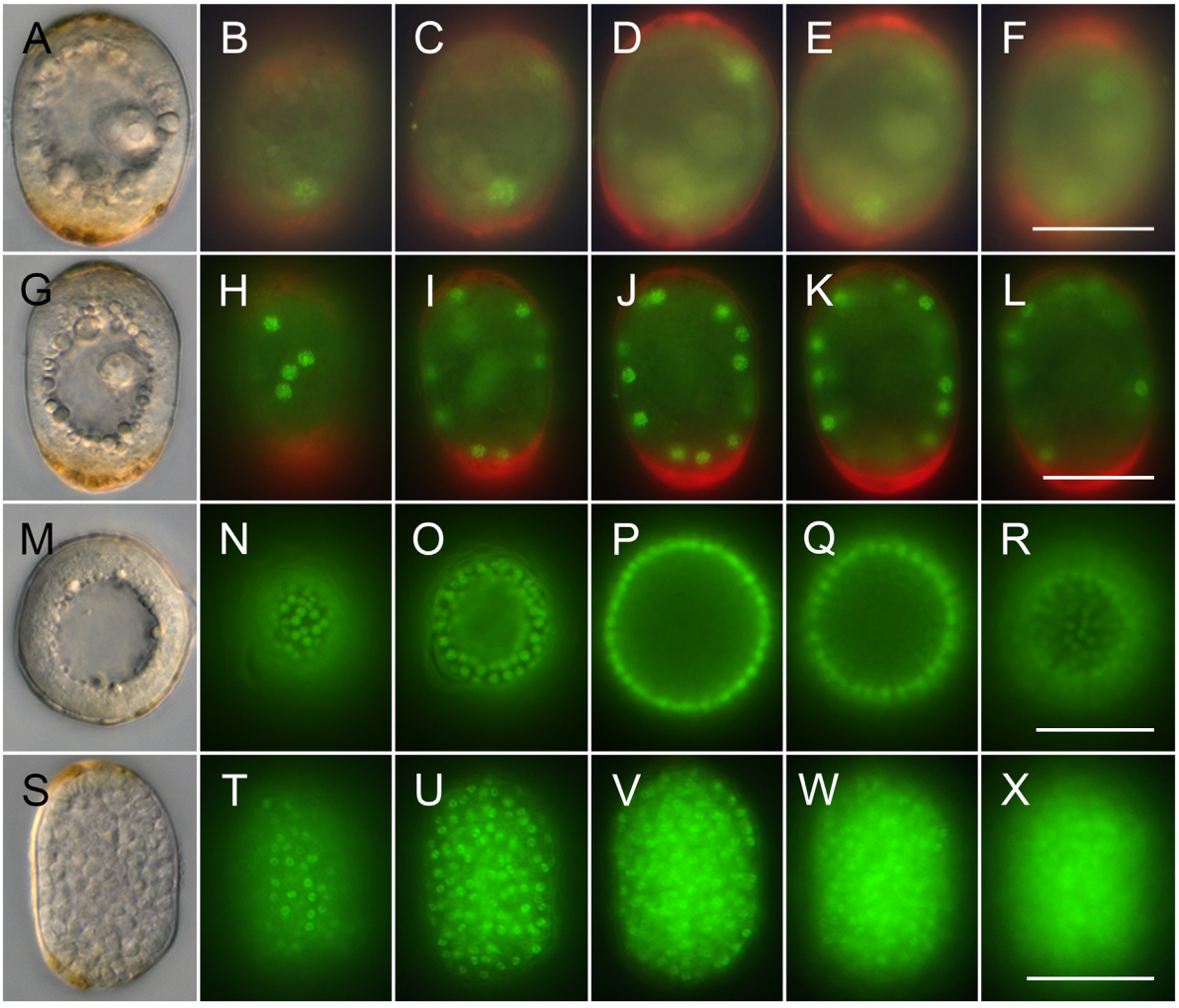

Figure 2. Differential interference contrast (DIC) and SYBR gold-stained epifluorescence images showing the distribution and division of nucleus during development stages of *Tuberlatum coatsi*. **A-F**. Micrographs of different focal (from a surface focus on the left side to deep focus on the right side) planes of the same early sporocyte (A) with SYBR gold-stained large nuclei. **G-L**. Micrographs of different focal planes of the same early to middle sporocyte (G) with several nuclei distributed along the cell periphery. **M-R**. Micrographs of different focal planes of the same middle sporocyte (M) with numerous nuclei densely distributed along the cell periphery. **S-X**. Micrographs of different focal planes of the same mature sporangium (S) full of numerous small nuclei. The scale bars in F, L, R, and X are 20 μm and apply to all panels.

ing the cytoplasmic content of the host. In the case of developments of multiple trophonts in a single host cell, their contact areas were somewhat bumpy (Fig. 4B). At this stage, a small-sized, non-condensed nucleus, lipid globules, and starch granules were observed. Once the host cytoplasm was completely consumed, the trophont then reached the size of the host in a single infection, although it was smaller if multiple trophonts developed within the same host at the same time. At this stage, the late trophont was characteristic of the presence of a large (approximately 5 μm), non-condensed nucleus without an apparent nucleolus at the periphery of the trophocyte, as well as a large vacuole containing amorphous hyaline material in the central area (Fig. 4C). The developing trichocysts and mitochondria were also observed at this stage (Fig. 4D, E).

At maturation of the trophont, the early sporocyte underwent karyokinesis, resulting in the production of multiple smaller nuclei without still apparent nucleoli or condensed chromatin along the periphery of the sporocyte (Fig. 5A). At this stage, the relatively short (approximately 5 μm) germ-tube(s)

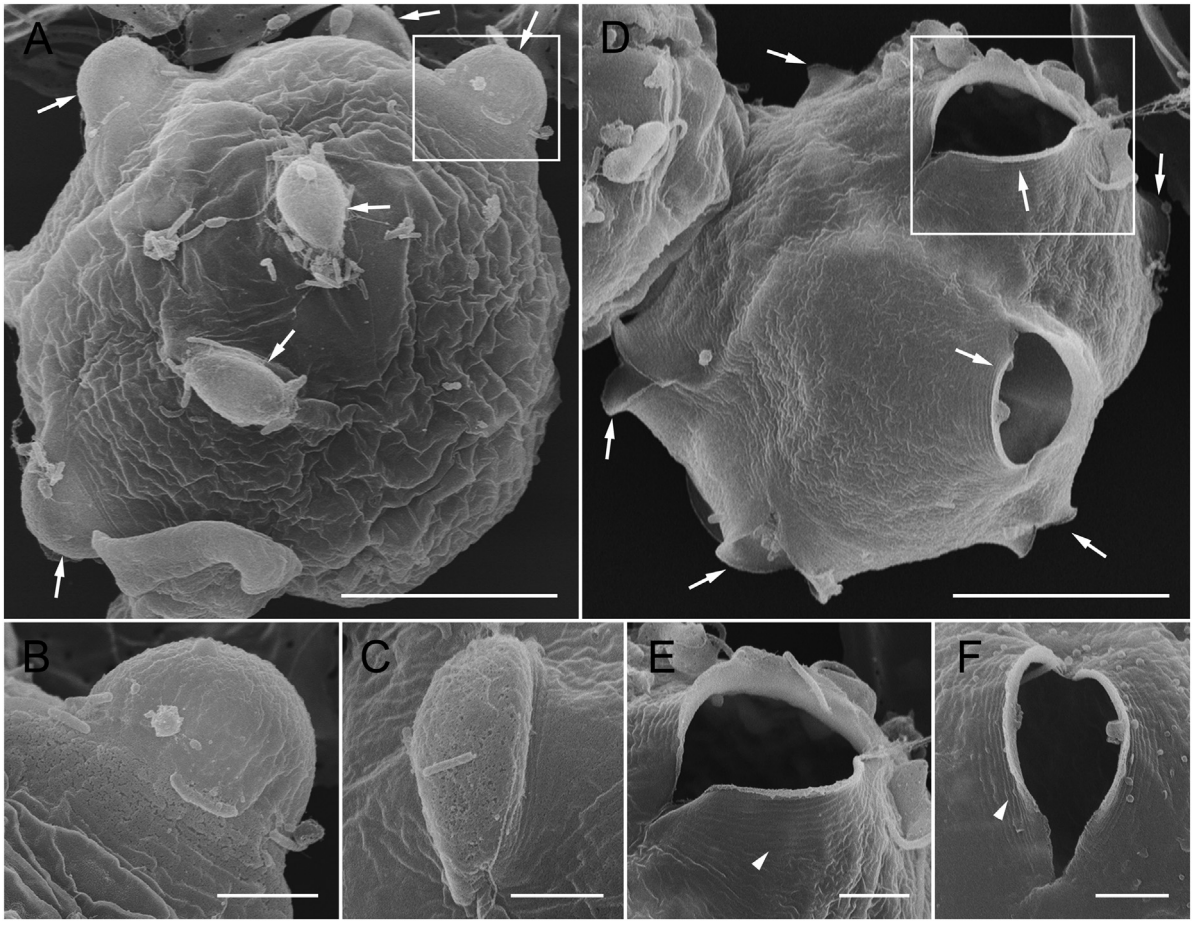

Figure 3. Scanning electron microscope (SEM) images showing the sporangium with short germ tubes of *Tuberlatum coatsi*. **A**. Sporangia with several closed germ tubes (arrows). **B**. Enlargement of the area indicated by the white box in **A** showing a closed germ tube in lateral view. **C.** The tip of a closed germ tube in top view. **D**. Sporangia with opened germ tubes (arrows). **E**. Enlargement of the area indicated by the white box in **D** showing opened germ tube. Note numerous wrinkles (arrowhead) around its opening. **F**. The opened germ tube showing biconvex lens shape in the top view along with wrinkles (arrowhead). Scale bars: A and D = 10 μm, B, C, E and F = 2 μm.

was formed (Fig. 5B), resulting from a swelling of the inner wall layer (see below). A large vacuole was still located in the central part of the sporocyte (Fig. 5A, B) and lipid globules and several organelles like mitochondria, Golgi apparatus, and bipartite trichocysts (i.e., consisting of two components, head and body) were present in the cytoplasm at the periphery of the sporocyte (Fig. 5C-E).

During the middle to late stages of development, a different degree of progression of nuclear development was observed: nuclei without condensed chromatin and nuclei with condensed chromatin distributed along the periphery (Fig. 6 A). Mitochondria, bipartite trichocysts, and micronemes were visible and flagellar were formed (Fig. 6B). With the initiation of cytokinesis, the zoospores began to differentiate from the periphery to the central direction of the sporocyte, with the amount of the central cytoplasm being reduced (Fig. 6C-E). The mature sporangium was filled with fully differentiated zoospores, each delimited by an independent plasma membrane (Fig. 6F). As the nucleus developed, the fibrous genetic materials began to aggregate along the margin of the nucleus and gradually became more condensed (Fig. 6G-J).

Development of the Sporangium Wall in *Tuberlatum coatsi*

At the earliest stages of infection, the parasitoid growing inside the parasitophorous vacuole was

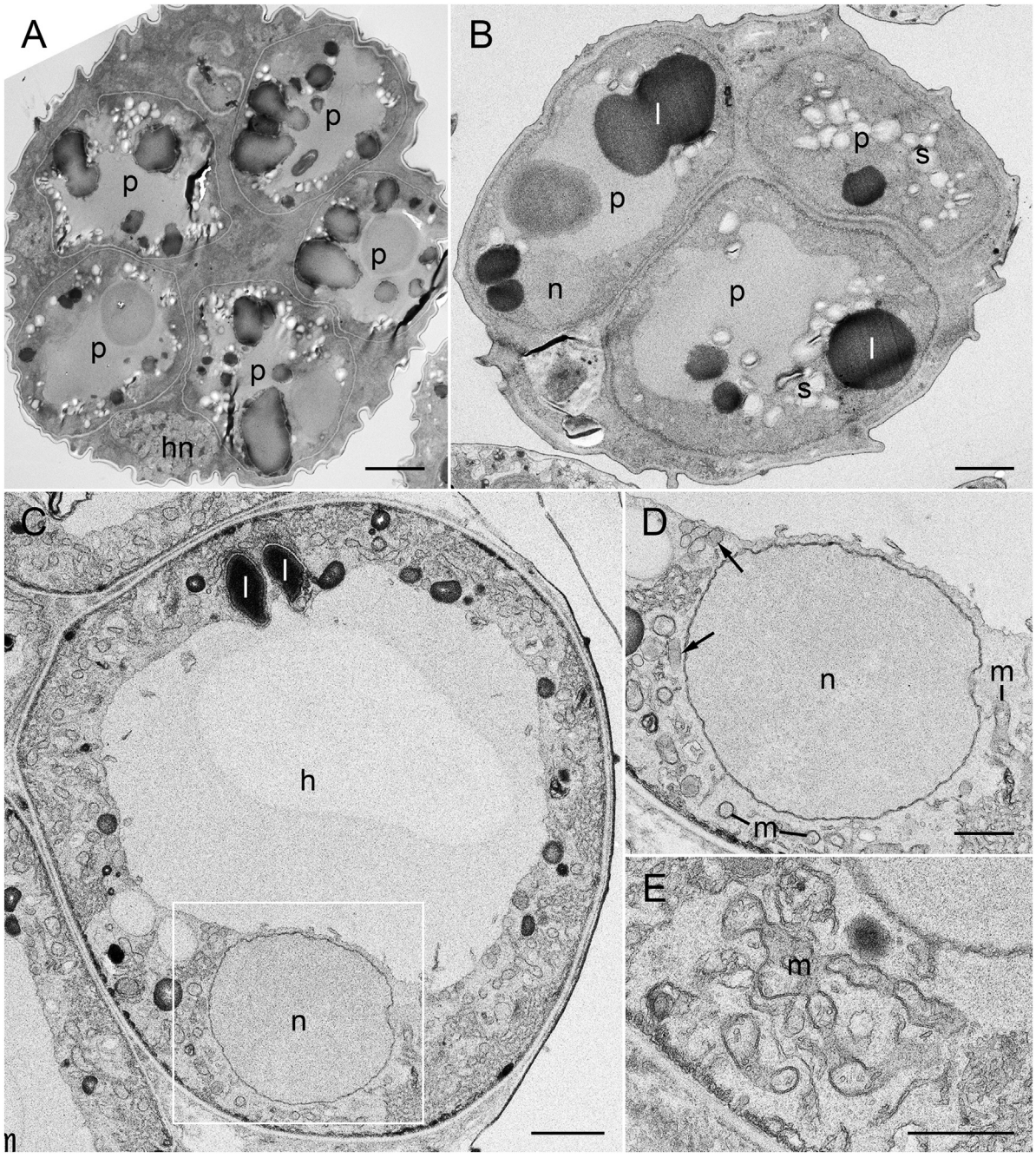

Figure 4. Transmission electron microscope (TEM) images of *Tuberlatum coatsi* during the early to late trophocyte stages. **A**. Five early trophonts (p) developing within the parasitophorous vacuoles in the early stage of infection. Degrading host nucleus (hn) is also visible. **B**. Three trophonts (p) in the middle stage of trophocyte. Note the bumpy contact area among them. The trophonts containing a nucleus (n), lipid globules (l), and starch granules (s). **C**. A trophont in late trophocyte stage containing central hyaline material (h), a large nucleus (n) and lipid globules (l). **D**. Enlargement of the area indicated by the white box in **C**, showing a nucleus with developing mitochondria-like (m) and trichocyst-like (arrows) bodies. **E**. Section clearly showing the developing mitochondria (m) at late trophocyte. Scale bars: A = 5 μm, B and C = 2 μm, D and E = 1 μm.

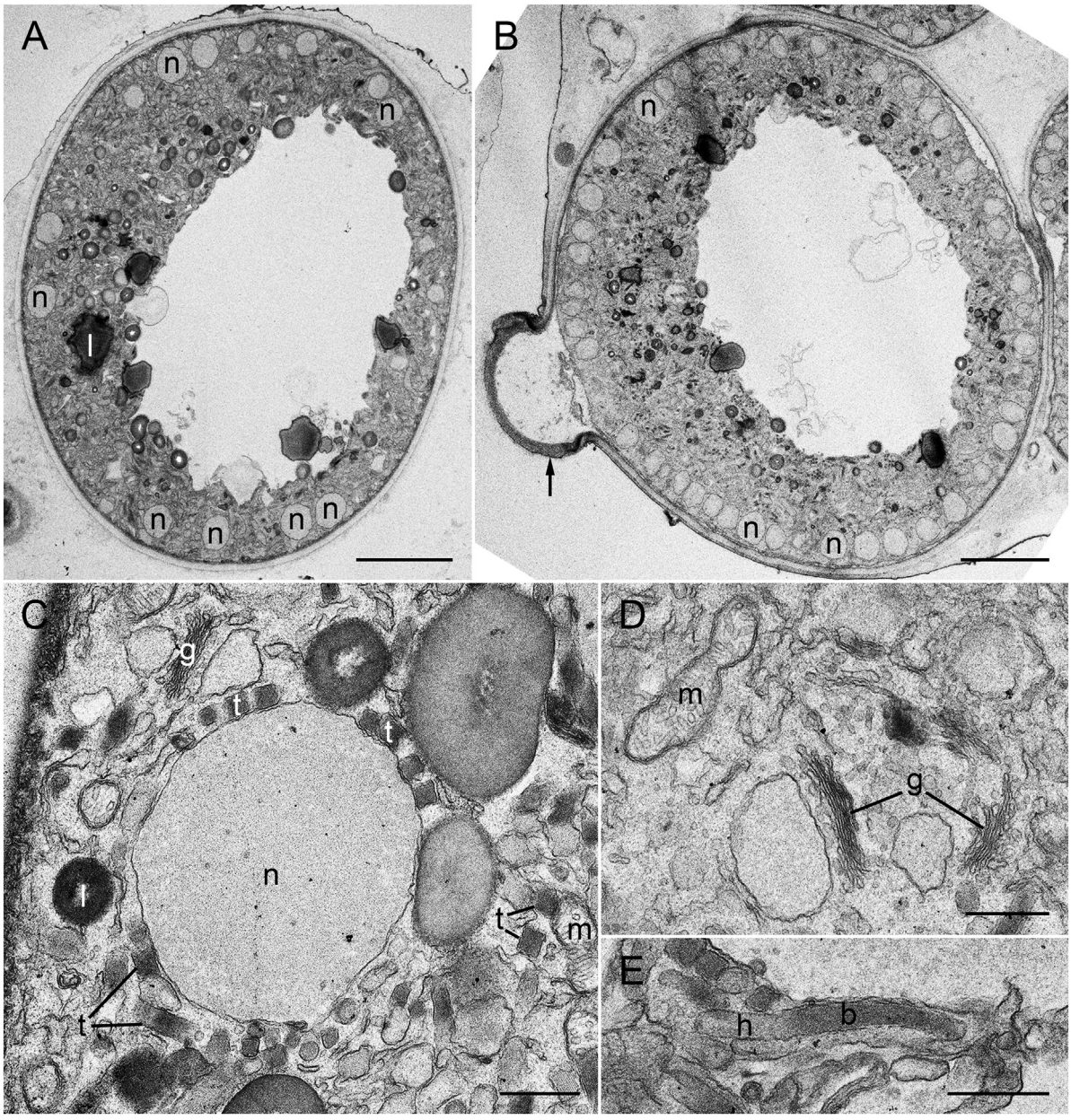

Figure 5. Transmission electron microscope (TEM) images of *Tuberlatum coatsi* during the early to middle sporocyte stage. **A**. The early sporocyte containing lipid globules (l), cytoplasmic content and several nuclei (n) distributed at the periphery of the cyst. **B**. The early to middle sporocyte, showing the developed germ tube (arrow) and a number of nuclei (n) distributed along the cell periphery. **C**. The nucleus without condensed chromatin in the early sporocyte, along with lipid globules (l), several trichocysts (t), and mitochondria (m). **D**. The parasitoid cytoplasm containing mitochondria (m) and Golgi apparatus (g) during the early to middle sporocyte. **E**. Longitudinal section showing the bipartite trichocyst consisting of the body (b) and the head (h). Scale bars: A and B = 5 μm, C-E = 0.5 μm.

separated from the host cytoplasm by an envelope consisting of three distinct layers: an inner convoluted membrane, a middle layer, and an outer wall layer (Fig. 7 A). As the trophont grew by consuming host cytoplasm, the middle layer gradually disappeared (Fig. 7B). At maturation, the trophont had a cyst wall consisting of two differentiated layers, an electron-dense inner wall layer and a less opaque outer wall layer (Fig. 7C). The surface of the cyst wall was smooth without processes or invagi-

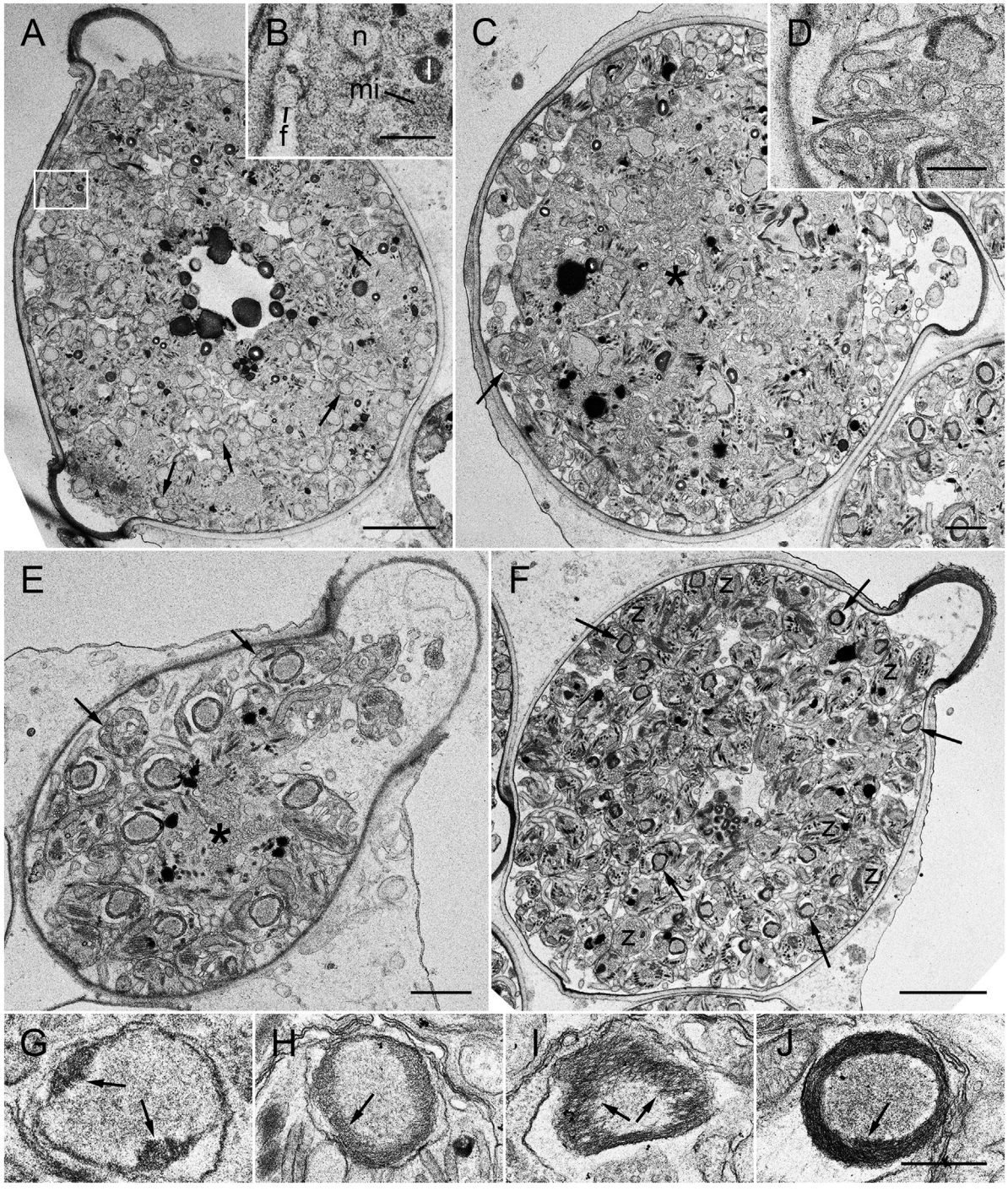

Figure 6. Transmission electron microscope (TEM) images of *Tuberlatum coatsi* during the middle to late sporocyte stage. **A**. The middle to late sporocyte showing numerous nuclei. Note the reduced central hyaline area and some nuclei having condensed chromatin (arrows) in their periphery at this stage. **B**. Enlargement of the area indicated by the white box in **A** showing flagellum (f), nucleus (n), lipid globule (l) and a cluster of micronemes (mi). **C**. The middle to late sporocyte showing the central undifferentiated cytoplasm (asterisk) and initiation of cytokinesis (arrow) for zoospore differentiation from the periphery to the central direction. **D**. Detail showing the invagination (arrowhead) at the periphery of the sporocyte. **E**. The late sporocyte showing some differentiated zoospores (arrows) from the central cytoplasm (asterisk). **F**. A sporangium full of numerous mature zoospores (z) with remarkable nuclei (arrows) having condensed chromatin. **G**. The nucleus of middle

nations. At the early stage of the sporocyte, the outer wall layer became thicker and the inner wall layer became more marked (Fig. 7D). At middle to late stages, the convoluted membrane began to invaginate and surround the immature zoospores, eventually acting as a source of the plasma membrane of each newly developed zoospore (Fig. 7E). At these stages, a sporangium having the inner wall layer as thick as the outer wall layer was sometimes observed (Fig. 7F). At early to middle stages when the germ-tube(s) developed, the inner wall layer began to swell, accompanied by the resultant breaking of the adjacent outer wall layer (Fig. 7G, H). The length of the germ-tube formed measured approximately 4 μm (Fig. 7I).

Zoospore of *Tuberlatum coatsi*

The zoospores were sigmoid shaped in lateral or ventral views (Fig. 8A, B) and were 2.8 ± 0.04 μm long and 1.39 ± 0.05 μm wide (n = 10, using SEM). The anterior area of the zoospore referred to a rostrum in lateral or ventral views (Fig. 8A, B). The zoospore possessed a posterior refractile body, which was easily visible under the light microscope (Fig. 8D). Each zoospore possessed two heteromorphic flagella, of which the hairy anterior flagellum, 6.13 ± 0.09 μm long (n = 6, using SEM), emerged ventrally from the cavity formed by the rostrum, encircled transversely its body, and terminated in a short conical tip (Fig. 8A-C). The posterior flagellum, 4.16 ± 0.11 μm long (n = 7, using SEM), emerged in between the anterior flagellum and the middle area of the body and ran longitudinally to the posterior end, and was characteristic of a proximal paraxial swelling and distal shrunken end (Fig. 8B, C).

Each zoospore contained the following major components: a posterior refractile body, lipid globules, several bipartite trichocysts consisting of an electron-dense body (square in cross section) and a twisted filamentous head, a large central mitochondrion with tubular cristae, alveoli, a Golgi body, and a rounded nucleus with condensed chromatin localized along its periphery (Fig. 9 A-C). Numerous micronemes were distributed over the central part of the cell from the posterior to the anterior end direction (Fig. 9A-C). The structure of the apical complex consisted of a pseudo-conoid formed by 4 microtubules in a curvilinear arrangement, micronemes with bulbous ends, and rhoptries (Fig. 9D-F). Conoid-associated micronemes were also observed (Fig. 9D). The axoneme of the hairy anterior flagellum had a heteromorphic pair of two central microtubules (Fig. 9G, I), whereas that of the posterior flagellum was not heteromorphic and rather was characteristic of the swelling (i.e., wing-like extension) (Fig. 9J). The basal body of the posterior flagellum did not contain a dense globule (Fig. 9H).

Phylogeny

The SSU rDNA sequence obtained for *T. coatsi* showed pairwise identities of a 92.3% to *D. pyriformis* sequence, a 90.4% to *S. prorocentri* sequence, an 84% to *P. rostrata* sequence, 80.2 ~ 81.2% to *P. infectans* sequences, and an 80.4% to *P. corolla* sequence. The partial LSU rDNA sequence from *T. coatsi* had an 80.2% similarity with that from *D. pyriformis* and 61.4 ~ 72% similarities with those from *Parvilucifera* species.

Molecular phylogenetic analysis, based on SSU rDNA sequences, revealed that Perkinsozoa forms a monophyletic group, with strong bootstrap support (ML, 100%) or a posterior probability (PP) of 1 (Fig. 10). The Perkinsozoa group was comprised of two separate clades, one containing *Perkinsus* spp. and a lot of marine and freshwater environmental sequences (45%/0.89), and the other containing Parviluciferaceae members and other marine and freshwater environmental sequences (62%/0.97). All sequences of the Parviluciferaceae members clustered together with moderate support (92%/1) and *D. pyriformis* diverged at the base of the group containing Parviluciferaceae members. *T. coatsi* was placed between *D. pyriformis* and *Snorkelia* spp. but had low statistical support (74%/0.99).

The combined SSU + LSU phylogeny (Fig. 11) also showed that the Perkinsozoa group was comprised of two separate clades, *Perkinsus* sp. and Parviluciferaceae members, with strong support (100%/1). All Parviluciferaceae members clustered together with strong support (100%1) and they

sporocyte containing partially condensed chromatin at its periphery (arrows). **H**. The nucleus of the middle to late sporocyte containing mostly condensed chromatin (arrow) at the periphery. **I**. The nucleus and condensed chromatin consisting of layers of very thin fiber-like materials (arrows). **J**. The nucleus of mature zoospore showing remarkable condensed chromatin at its periphery (arrow). Scale bars: A and C = 5 μm, B = 2 μm, D = 1 μm, E-I = 0.5 μm.

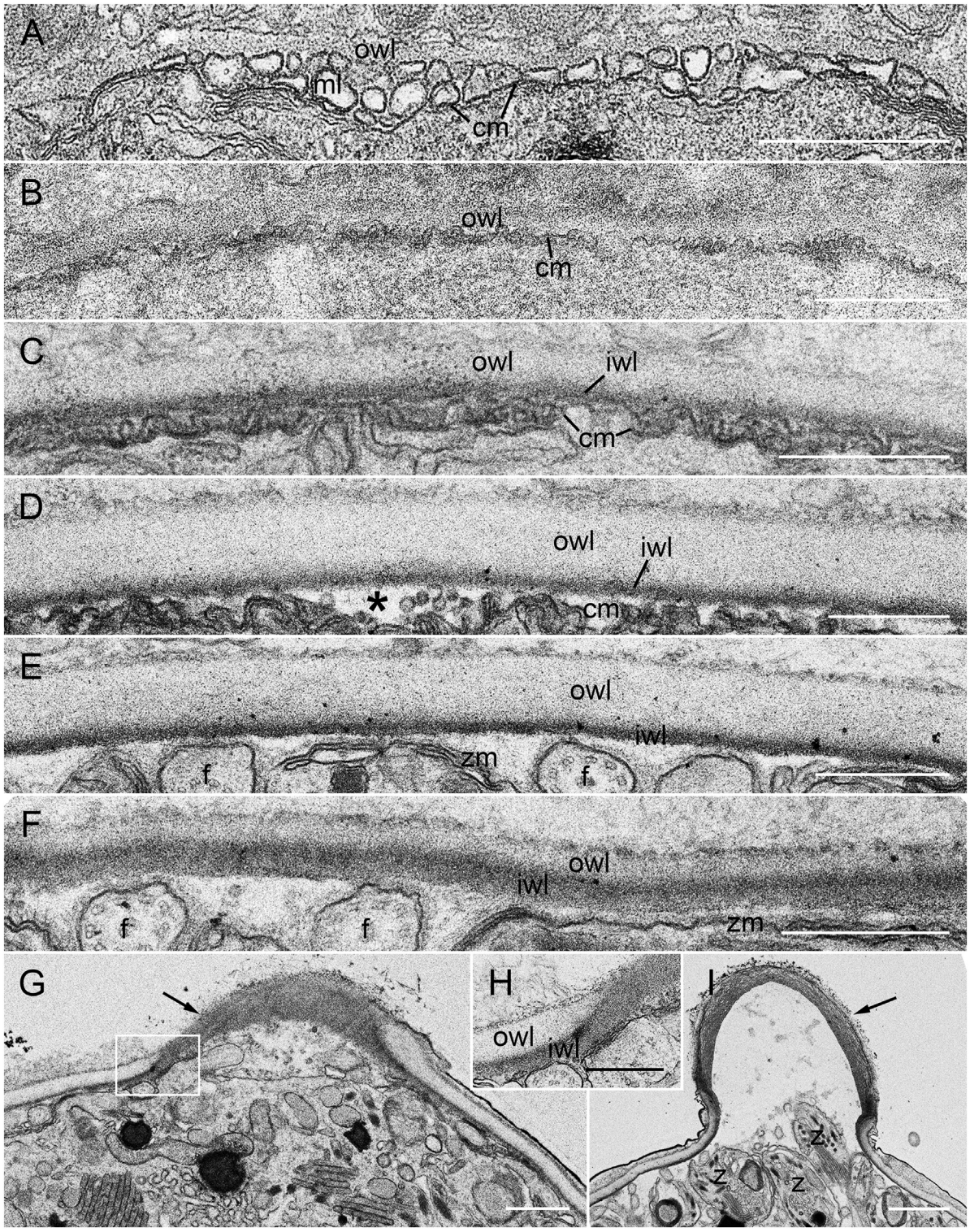

Figure 7. Transmission electron microscope (TEM) images of cyst walls for the different stages of *Tuberlatum coatsi*. **A**. The cyst wall of the early trophocyte consisting of an inner convoluted membrane (cm), a middle layer (ml), and an outer wall layer (owl). **B**. The cyst wall of the middle to late trophocyte consisting of the convoluted membrane (cm) and the outer wall layer (owl). Note that the middle layer gradually disappeared as the trophont grew by consuming host cytoplasm. **C**. The cyst wall of the late trophocyte consisting of two layers: an inner

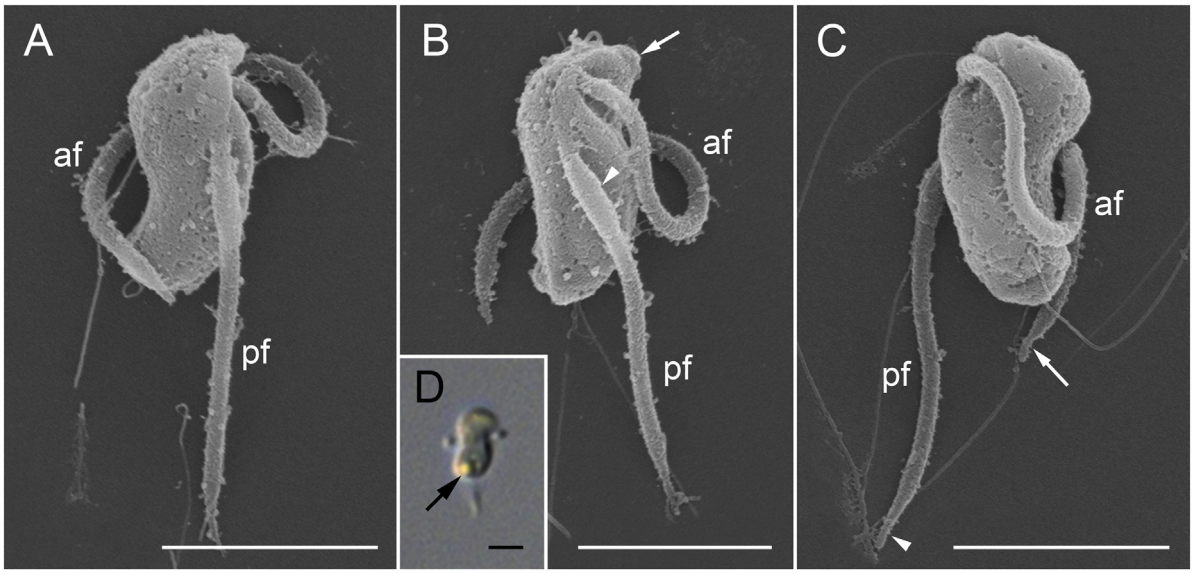

Figure 8. Scanning electron microscope (SEM) (A-C) and differential interference contrast (D) images of the zoospore of *Tuberlatum coatsi*. **A**. Lateral view of zoospore showing the anterior flagellum (af) encircling the cell and the posterior flagellum (pf) running to the posterior end of the cell. **B**. Ventral view of zoospore showing the anterior flagellum (af) emerging in the cavity formed by the rostrum (arrow) and the posterior flagellum (pf) with proximal paraxial swelling (arrowhead). **C**. Dorsal view of zoospore showing the anterior flagellum (af) with short conical tip (arrow) and the posterior flagellum (pf) with the shrunken distal end (arrowhead). **D**. Zoospore containing a refractile body at the posterior end of the cell (arrow). All scale bars = 2 μm.

were comprised of two separate clades, one containing *Parvilucifera* species (100%/1), and the other containing *T. coatsi*, *Snorkelia* spp., and *D. pyriformis* (60%/0.84). *T. coatsi* diverged from the group consisting of *Snorkelia* spp. and *D. pyriformis*, but the branch was poorly supported (45%/0.52) in the phylogenetic analysis using the current dataset.

Taxonomic Summary

Alveolata Cavalier-Smith, 1991

Myzozoa Cavalier-Smith and Chao, 2004

Perkinsozoa Norén and Moestrup, 1999

Parviluciferaceae Reñé and Alacid, 2017

Tuberlatum Jeon et Park gen. nov.

Diagnosis

Parviluciferaceae with two to four short (~4.7 μm long) and wide (8 ~ 15.4 μm at the base) germ tubes in a sporangium. The germ tubes are dome-shaped in lateral view. The opened germ tubes resemble biconvex lens in shape in top view and are characterized by numerous wrinkles around their openings. Sporangium wall is composed of 2 layers and is relatively thick compared to that of *Parvilucifera* species.

Type species

---

wall layer (iwl) and an outer wall layer (owl), with the convoluted membrane (cm). **D**. The cyst wall at an early stage of the sporocyte, showing the thicker outer wall layer (owl) and the more marked inner wall layer (iwl), with the convoluted membrane (cm) partially detached from the cyst wall (asterisk). **E**. Early invagination of the convoluted membrane to surround the immature zoospores (zm), eventually acting as a source of the plasma membrane of each newly developed zoospore, at the middle to late sporocyte. Flagella (f) are also shown. **F**. Inner wall layer as thick as the outer wall layer was sometimes observed. **G**. The early to middle sporocyte showing the developing germ tube (arrow). **H**. Enlargement of the area indicated by the white box in **G**. Note the accompanied breaking of adjacent outer wall layer (owl) during the swelling process of the inner wall layer (iwl). **I**. Fully developed germ tube (arrow). Zoospores (z) are also shown. Scale bars: A-F and H = 0.5 μm, G = 1 μm, I = 2 μm.

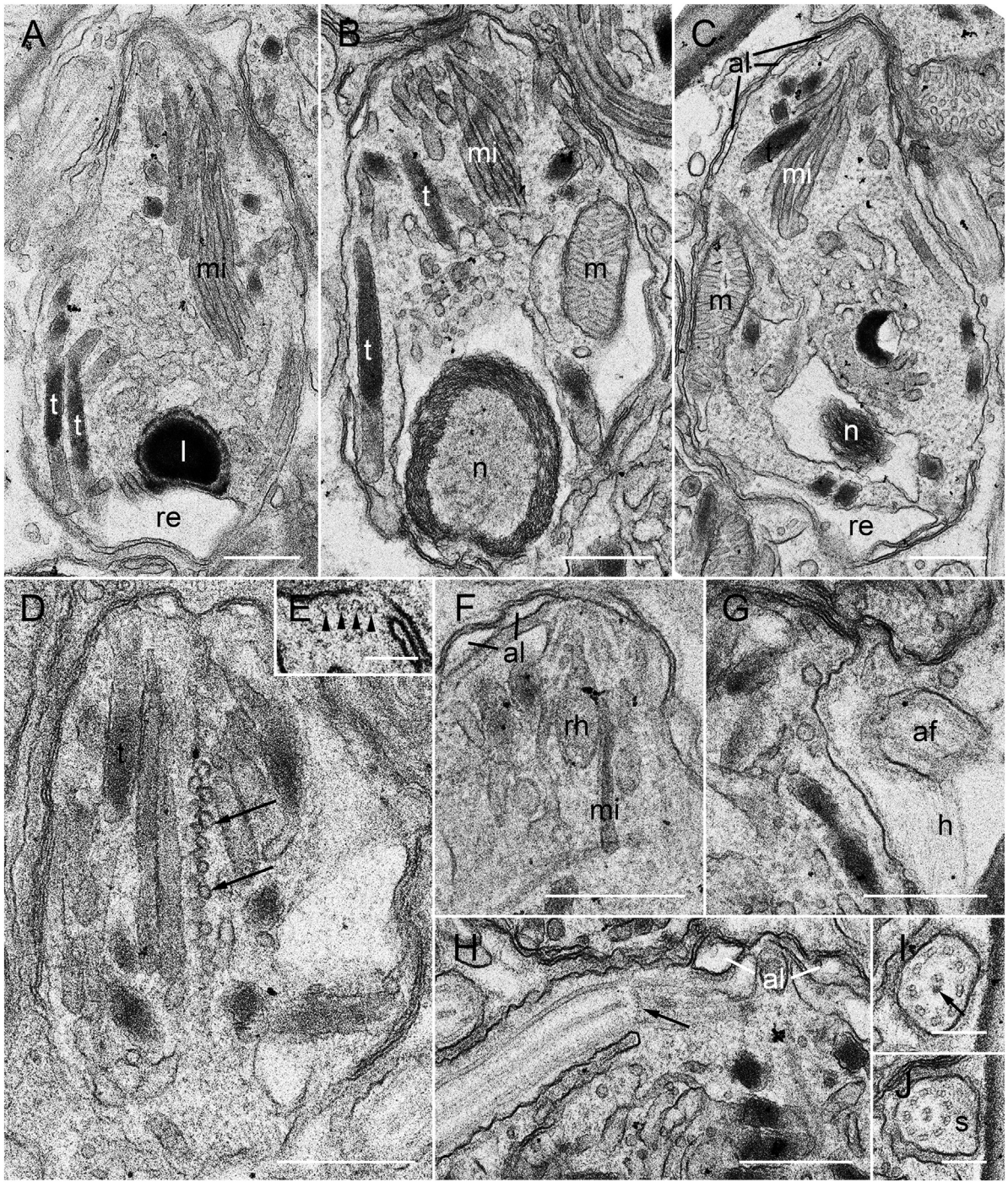

Figure 9. Transmission electron microscope (TEM) images of the zoospore of *Tuberlatum coatsi*. **A**. Longitudinal section showing the zoospore containing the cluster of micronemes (mi), several bipartite trichocysts (t), lipid globule (l), and the refractile body (re). **B**. Section showing zoospore containing a nucleus with condensed chromatin at its periphery (n), the cluster of micronemes (mi), several bipartite trichocysts (t), and mitochondrion with tubular cristae (m). **C**. Section showing zoospore containing the cluster of micronemes (mi), mitochondrion with tubular cristae (m), alveoli (al), nucleus (n), and refractile body (re). **D**. Section showing the termination of the conoid-associated micronemes (arrows) in zoospore. **E**. Section showing the conoid consisting of four microtubules (arrow heads). **F**. Section showing the alveoli (al) and the apical complex consisting of the rhoptry (rh) and microneme with the bulbous posterior end (mi). **G**. Section through an anterior area of the zoospore

Tuberlatum coatsi sp. nov.

Etymology

Genus name is the combination from the Latin neuter noun singular *Tuber*, referring to bump or swelling of the surface of sporangium, and the Latin neuter nominative adjective *latum* meaning wide.

Tuberlatum coatsi Jeon et Park sp. nov.

Diagnosis

Two to four dome-shaped, short germ tubes for the release of zoospores from a single sporangium are present. Zoospores are sigmoid shaped in lateral and ventral views and possess a posterior refractile body.

Holotype

Both platinum sputter-coated SEM stub and resin-embedded used for TEM of all life-cycle stages of parasites have been deposited in the National Marine Biodiversity Institute of Korea, Republic of Korea under the code MABIK PR00043202 to PR00043204 and MABIK PR00043205 to PR00043215, respectively.

Type locality

Gangsa Harbor, Pohang, Korea, East Sea (36°02′23″N 129°34′45″E).

Etymology

The species is named after Dr. D. Wayne Coats, who has greatly contributed to the taxonomy of the parasites of marine protists, especially ciliates and dinoflagellates.

Discussion

Since the first description of *P. infectans* by Norén et al. (1999), the family Parviluciferaceae has long contained only one species in the genus *Parvilucifera* until Leander and Hoppenrath (2008) reported *P. prorocentri*, a parasitoid infecting the marine benthic dinoflagellate *Prorocentrum fukuyoi*. At that time, another parasitoid (*P. sinerae*) was also described (Figueroa et al., 2008), but later it was revealed to be the same species as *P. infectans* when based on morphological, ultrastructural, and molecular data (Jeon et al. 2018). While describing *P. prorocentri*, Leander and Hoppenrath (2008) also clearly recognized that it differs significantly from *P. infectans* in many respects (e.g. germ tube formation and the presence of bipartite trichocysts), but did not erect a new genus for this parasitoid because available information regarding Perkinsozoa biodiversity was not sufficient at the time. Recently, three more parasitoids infecting marine dinoflagellates, *P. rostrata*, *P. corolla*, and *D. pyriformis*, were formally described (Lepelletier et al. 2014; Reñé et al. 2017a,b). Now, the result from the present study also expands species diversity in the family Parviluciferaceae by adding a novel parasitoid, *Tuberlatum coatsi*.

Tuberlatum coatsi examined in this study shares many characters in common with other members of Parviluciferaceae, including the use of dinoflagellates as hosts, the overall life-cycle patterns, its development inside the host, and even many ultrastructural characters (Table 1). Nonetheless, it shows some remarkable differences from other Parviluciferaceae members, including the presence of 2 ~ 4 dome-shaped, short germ tubes. To erect the new genus *Dinovorax*, Reñé et al. (2017a) described it as follows: "*Endoparasitoid of dinoflagellates. Sigmoid shaped zoospores penetrate a healthy host and transform into the feeding stage (trophont). Zoospores are biflagellated, with both flagella equal in size but heteromorphic. Both emerge from the anterior half of the cell. When the host is consumed, the trophont forms a germ-tube and transforms into a sporocyte. Numerous new zoospores are then produced and released through the germ-tube once completely formed.*" Furthermore, while erecting the genus *Dinovorax*, they also moved *Parvilucifera prorocentri* to the genus *Snorkelia*, by newly describing this genus as follows: "*Endoparasitoid of dinoflagellates. It forms a germ-tube from where zoospores are released. Zoospores are reniform. The nucleus has condensed chromatin beneath the nuclear envelope. A refractile body and bipartite trichocysts are present. They possess two heteromorphic flagella, a short*

showing the anterior flagellum (af) with its hairs (h). **H**. Section showing the alveoli (al) and the basal body in longitudinal section containing a transverse septum in the transition zone (arrow). **I**. Transverse section of the axoneme of anterior flagellum showing a heteromorphic pair of central microtubules (arrow). **J**. Transverse section of the axoneme of posterior flagellum showing a paraxial swelling (s). Scale bars: A-D and F-H = 0.5 μm, E = 0.1 μm, I and J = 0.2 μm.

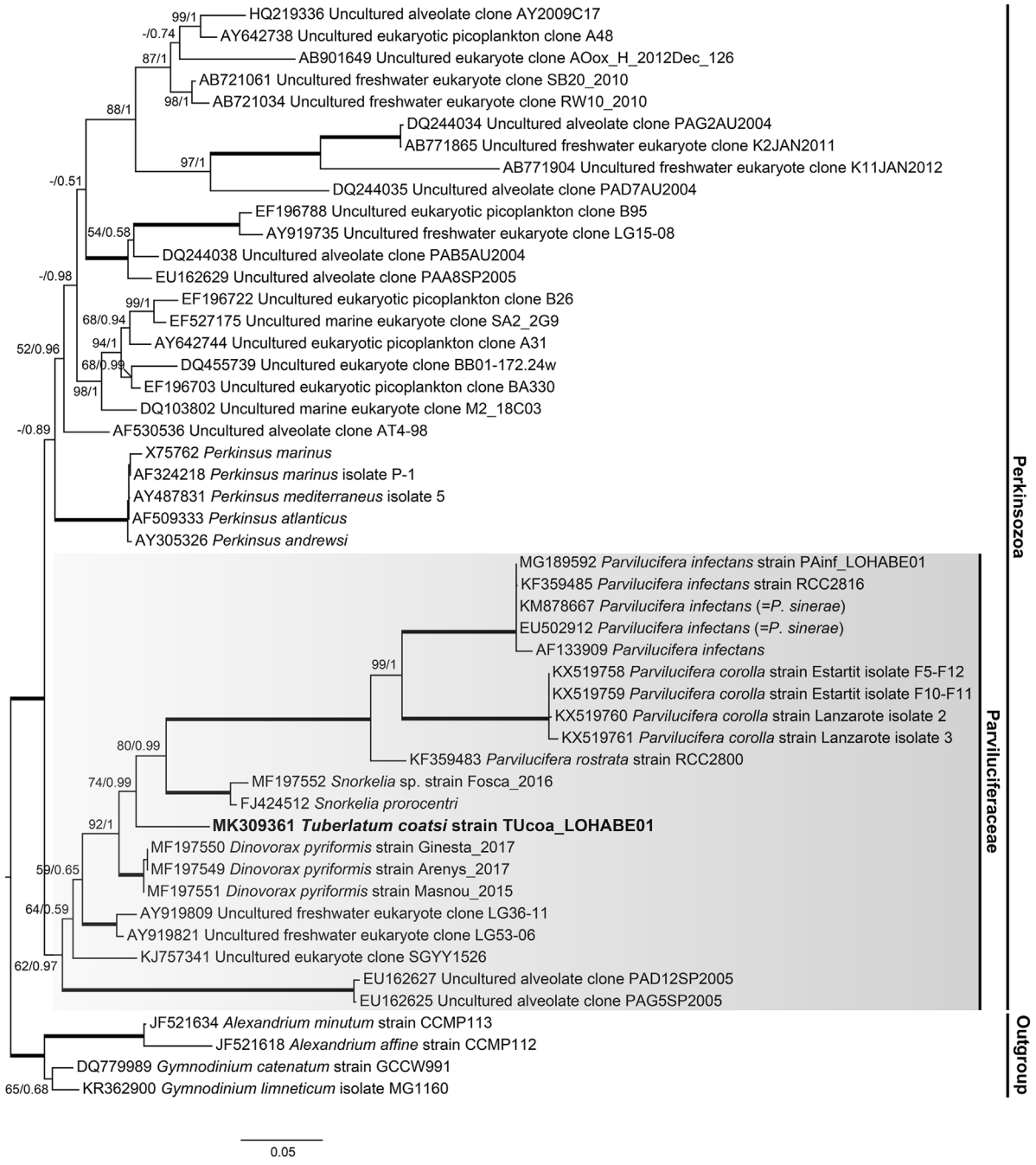

Figure 10. Maximum likelihood phylogenetic tree inferred from small subunit rRNA gene sequences (1585 bp). Sequences of the dinoflagellates *Alexandrium* spp. and *Gymnodinium* spp. were used as the outgroup. The sequence for *Tuberlatum coatsi* in the present study is indicated in bold. The shaded area indicates Parviluciferaceae members. Numbers shown on nodes are support values of bootstrap percentages (left) using RAxML fast bootstrapping analysis and Bayesian posterior probabilities (right) higher than 50% and 0.5, respectively. Thick lines indicate support values of 100% and 1 pp.

Table 1. Comparison of the morphological characters of *Tuberlatum coatsi* with other Parviluciferaceae members and *Perkinsus* spp.

		T. coatsi (This study)	*D. pyriformis* (Reñé et al. 2017a)	*S. prorocentri* (Leander and Hoppenrath 2008)	*P. rostrata* (Lepelletier et al. 2014)	*P. infectans* (=*P. sinerae*) (Figueroa et al. 2008; Garcés and Hoppenrath 2010; Jeon et al. 2018; Lepelletier et al. 2014; Norén et al. 1999)	*P. corolla* (Reñé et al. 2017b)	*Perkinsus* spp. (Azevedo 1989; Casas et al. 2004; McLaughlin et al. 2000)
Trophocyte	Trophocyte location	Host cytoplasm	Host cytoplasm	Host cytoplasm	Host cytoplasm	Host cytoplasm	Host cytoplasm	Host tissues
	Large nucleus	Y	Y	Y	Y	Y	Y	Y
	Lipid droplets	Y	Y	Y	Y	Y	Y	Y
Sporocyte	Hyaline material	Y	Y	Y	Y	Y	Y	Y
	Residual body	Y	Y	N	Y	Y	Y	?
	Length of processes (μm)	absence	absence	absence	0.4	0.4 ~ 0.8	0.3 ~ 0.7	absence
	Number of sporangium wall layer	2	2	2	4	4	4	4
	Sporangium wall (μm)	0.33	0.35	0.34	*0.19/0.64	*0.24/0.68	*0.2/0.65	1.8 ~ 3.5
	Structure of the release path of zoospores	germ tube	germ tube	germ tube	aperture	aperture	aperture	germ tube
	Number of the release path of zoospores	2 ~ 4	1	1	several	several	several	1 ~ 2
	Length of the germ tube (μm)	2.7 ~ 4.7	10 ~ 15	10 ~ 15				2.5 ~ 17.3
	Sporangium diameter (μm)	19 ~ 34 (in *Alexandrium catenella*)	19.4 ~ 22? (in *Prorocentrum micans*)	20 ~ 25 (in *prorocentrum fukuyoi*)	?	11 ~ 72 (depends on host size)	?	20 ~ 135
	Ratio of germ tube length relative to sporangium diameter	1:8	1:1.65	1:1.8				1:3 ~ 1:6

	Opening shape of the germ tube	biconvex	circular	circular				circular
	Diameter of the germ tube (μm)	8. ~ 15.9 in major axis; 3.8 ~ 6.8 in minor axis (in *Alexandrium catenella*)	3.4 ~ 5	4 ~ 5				6.8 ~ 13[a]/ 26 ~ 27[b]
	Sporangium shape	variable	pear		sphere	sphere	sphere	sphere
Zoospore	Zoospore shape	sigmoid	sigmoid	reniform	elongated	elongated	teardrop	Ellipsoidal
	Zoospore length (μm)	2.8	6	4	6 (±0.5)	4 ~ 5.5/2.7[c]	2.9 (± 0.4)	3.7 ~ 4.5
	Zoospore width (μm)	1.3	3	1.5	1.8 (± 0.2)	1 ~ 1.6/2.2[c]	1.7 (± 0.4)	2.4 ~ 2.9
	Zoospores/10^3um^3	111 ± 7.5 (n = 6)	10 ~ 16 (n = 4)	?	?	44.9 ± 1.5 (n = 38)[d]	?	?
	Anterior flagellum (μm)	6.1 (± 0.1)	both flagella are similar in length	longer flagellum	2 ~ 3 time longer than cell body	12.7 ~ 15/7[c]	up to 13.5	12.7[e]/5.5[a]
	Posterior flagellum (μm)	4.1 (± 0.1)		shorter flagellum	as long as the body	2.2 ~ 2.7/1.5[c]	3.5 ~ 4	10.7[e]/3[a]
	Hairs of anterior flagellum	Y	Y	?	Y	Y	Y	?/Y[a]
	Swelling of posterior flagellum	Y	?	?	Y	Y	?	?

Table 1 (*Continued*)

	T. coatsi (This study)	*D. pyriformis* (Reñé et al. 2017a)	*S. prorocentri* (Leander and Hoppenrath 2008)	*P. rostrata* (Lepelletier et al. 2014)	*P. infectans* (=*P. sinerae*) (Figueroa et al. 2008; Garcés and Hoppenrath 2010; Jeon et al. 2018; Lepelletier et al. 2014; Norén et al. 1999)	*P. corolla* (Reñé et al. 2017b)	*Perkinsus* spp. (Azevedo 1989; Casas et al. 2004; McLaughlin et al. 2000)
Dense globule in the basal body	N	N	N	Y	Y	Y	Y
Heteromorphic pair of central microtubules in anterior axoneme	Y	Y	Y	Y	Y	Y	Y
Refractile body	Y	N	Y	Y	Y	Y	Y
Alveoli	Y	Y	Y	Y	Y	Y	Y
Bipartite trichocysts	Y	Y	Y	N	N	N	N
Condensed genetic material in zoospore nucleus	Y	Y	Y	Y	Y	Y	Y
Condensed genetic material distribution	peripheral	Ovoid bodies	peripheral	peripheral	peripheral	peripheral	peripheral
Micronemes	Y	Y	Y	Y	Y	Y	Y
Reduced pseudoconoid	4	4	4∼5	5	5	4∼5	Y
Conoid-associated micronemes	Y	?	Y	Y	Y	Y	Y
Rhoptries	Y	Y	?	Y	Y	Y	Y

*Wall thickness without and with transparent layer.
[a]McLaughlin et al. (2000).
[b]Casas et al. (2004).
[c]Figueroa et al. (2008).
[d]Jeon et al. (2018).
[e]Azevedo (1989).

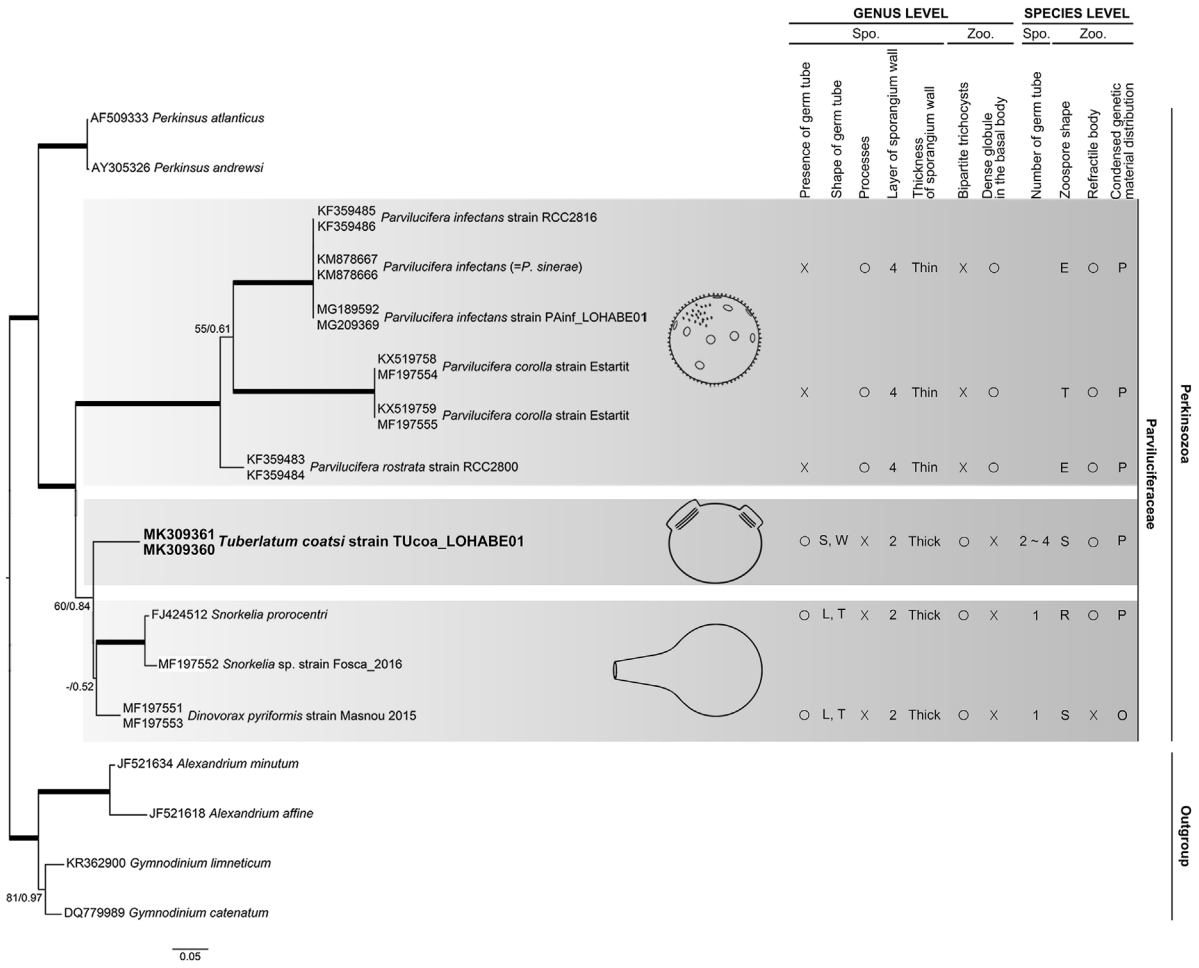

Figure 11. Maximum likelihood phylogenetic tree inferred from the concatenated of small and large subunit rRNA gene sequences (2672 bp). Sequences of the dinoflagellates *Alexandrium* spp. and *Gymnodinium* spp. were used as the outgroup. In the phylogenetic analysis, the sequences of *Snorkelia* spp. contained the only small subunit rRNA gene sequences because the large subunit rRNA gene sequences were at present not available. The sequences for *Tuberlatum coatsi* in the present study are indicated in bold. Some key morphological characters for Parviluciferaceae members at the genus and species levels are mapped together on the tree. Numbers shown on nodes are support values of bootstrap percentages (left) using RAxML fast bootstrapping analysis and Bayesian posterior probabilities (right) higher than 50% and 0.5, respectively. Thick lines indicate support values of 100% and 1 pp. Abbreviations: elongated (E), long & thin (L, T), ovoid bodies (O), peripheral (P), reniform (R), sigmoid (S), short & wide (S, W), teardrop (T).

posterior flagellum short and a haired anterior one. Apical complex is present, with pseudo-conoid, micronemes and rhoptries." From their work, we did not see any reasons to split into two different genera *Dinovorax* and *Snorkelia* for species with a germ-tube, except that the two species were placed paraphyletically at the base of the *Parvilucifera* species in their phylogenetic analysis (Reñé et al. 2017a). Those diagnoses used for *Dinovorax* and *Snorkelia* are not only in part highly general enough to be considered at taxonomic levels higher than genus (e.g., an endoparasitoid of dinoflagellates), but also are in part not specific enough to appropriately sort species belonging to the Parviluciferaceae at the species level. This our argument is also supported by comparison of morphological and ultrastructural characters among the Parviluciferaceae members (Table 1). For example, both genera *Dinovorax* and *Snorkelia* are most distinguishable from the genus *Parvilucifera* by the presence of germ-tube in sporangium but share this pronounced morphological character, which in

turn makes it difficult to sort the two genera with a germ-tube. The refractile body is present in all the members of Parviluciferaceae but *D. pyriformis*, suggesting that it is not an appropriate diagnostic character at the genus level. The ultrastructural characters, including pseudo-conoid, micronemes, and rhoptries, are also present in all Parviluciferaceae members, again suggesting that these are not appropriate diagnostic characters at the genus level.

Recent subsequent discoveries of Parviluciferaceae members along with the new parasitoid found in this study raise the need to appropriately sort them, in particular at the genus level. The presence and absence of germ tube and its shape, presence or absence of process in sporangium, the thickness of sporangium wall, bipartite trichocysts, and a dense globule in the basal body in zoospore ultrastructures are appropriate morphological diagnostic chatacters available at the genus level in the family Parviluciferaceae (Fig. 11). For example, sporangium in species belonging to the genus *Parvilucifera* lacks germ tube(s) and is ornamented with numerous processes at the surface, its wall thickness is relatively thin (0.19-0.24 μm without transparent layer), and a dense globule in the basal body is present in all of their zoospores. By contrast, species within genera *Tuberlatum* and *Dinovorax* are different from *Parvilucifera* species in that they develop germ tube(s), have thick (0.33-0.35 μm) sporangium wall, and have bipartite trichocysts in zoospores. The main difference between *Tuberlatum* and *Dinovorax* is in the shape of the germ tube(s); whereas the former develops short (1:8; mean ratio between the length of the germ tube and the diameter of the sporangium) and wide (8–16 μm), two to four, germ tubes, the latter develops a long (1:1.65; mean ratio between the length of the germ tube and the diameter of the sporangium) and thin (3.4–5 μm) germ tube. Concerning the species with the formation of germ tube(s), separation into two genera (*Tuberlatum* and *Dinovorax*) seems to be more or less conservative when considering the recent rapid increase in species diversity in the family Parviluciferaceae. Given such a difference between the above two genera, it would be advisable to move species within the genus *Snorkelia* to genus *Dinovorax* in the future, according to the page precedence in the original reference (Reñé et al. 2017a). Closer examination in this study revealed that the zoospore shape, refractile body, and distribution of condensed genetic material in the nucleus of zoospore are diagnostic, which could be used to sort species within *Dinovorax*/*Snorkelia* at the species level (Fig. 11).

Among the Parviluciferaceae members, it appears almost impossible to distinguish *Parvilucifera* species only based on the morphological characters as they share many morphological characters in common with each other at both the genus and species levels (Fig. 11, Table 1). As far as we know, the teardrop shape of zoospores from *P. corolla* is the only morphological diagnostic that differs significantly from other *Parvilucifera* species (*P. infectans* and *P. rostrata*) with an elongated shape. Apart from the genetic differences, thus, the appropriate morphological characters for easily sorting *Parvilucifera* species should be searched for in the future.

The attempts to infer evolutionary trends in Perkinsozoa characters have previously been made through comparisons of morphological and ultrastructural features, as well as phylogenetic analyses (Hoppenrath and Leander 2009; Reñé et al. 2017a). Parviluciferaceae members and Perkinsus species appear to have evolved independently from a common ancestor. The presence of germ-tube(s) in sporangium has been considered as an ancestral character of the common ancestor (Hoppenrath and Leander 2009; Reñé et al. 2017a). In addition, previous phylogenetic analyses showed that the genera *Dinovorax* and *Snorkelia* occupy a basal position and species belonging to the genus *Parvilucifera* occupy a terminal position in the family Parviluciferaceae (Reñé et al. 2017a). For these reasons, it seems to be tempting to consider that *Parvilucifera* species are more evolved ones within Parviluciferaceae compared to genera *Dinovorax* and *Snorkelia* (Reñé et al. 2017a). However, the finding of new species with short germ-tubes and its morphological comparison with the extant species, and phylogenetic analysis based on the concatenated SSU and LSU rDNA data in the present study suggest that a common ancestor of Parviluciferaceae members has evolved independently into two distinct clades: one containing *Parvilucifera* species and the other consisting of *Tuberlatum*, *Dinovorax*, and *Snorkelia*. For example, the germ-tube(s) that a common ancestor posessed were independently lost in the clade containing *Parvilucifera* species. By comparison, in the clade consisting of *Tuberlatum*, *Dinovorax*, and *Snorkelia*, it seems to be evolved from sporangium with several short germ-tubes to sporangium with a single long germ-tube. What kind of ecological and/or biological advantages the parasitoids get from such a advanced morphology (i.e. multiple apertures or a single long germ-tube for the release of zoospores) remain unknown at present. The more new species are found in the future,

the more knowledge of Perkinsozoa biodiversity as well as their character evolution will greatly increase.

Methods

Parasitoid isolation and cultures: Concentrated seawater samples were collected using a 20 μm mesh plankton net through vertical towing from the bottom to the surface (0 ∼ 4 m) on June 2017 in Pohang (36°02′23″N, 129°34′45″E), Korea. The live samples were first filtered through a 200 μm mesh to remove the large zooplankton grazers and transferred to the laboratory. In the concentrated sample collected from Pohang, the dominant dinoflagellates were *Alexandrium* sp., *Ceratium fusus*, *C. furca*, *Dinophysis* spp. and *Scrippsiella* sp. From the concentrated live sample, aliquots (2 mL) were distributed into a 6-well plate (Corning, New York, USA) containing a total volume of 1 mL of the mixed dinoflagellates (*Alexandrium catenella* strain Ac-LOHABE01 and *Scrippsiella* sp. strain Ss-LOHABE03) as potential hosts at 20 °C under a 14:10 h light:dark cycle with cool-white fluorescent light providing 100 μmol photons m^{-2} s^{-1}. After 2 days of incubation, the rounded trophonts characteristic of the parasitoids were observed from the dinoflagellates *A. catenella* and *Scrippsiella* sp. Then, the infected host cells were isolated using a drawn glass micropipette under an inverted microscope (Axio Vert.A1, Carl Zeiss Inc., Hallbergmoos, Germany), washed six times in syringe filtered seawater from the samples (0.45 μm pore size; Advantec, Tokyo, Japan) to prevent contamination, and then individually transferred to a 96-well plate (Corning, New York, USA) containing 30 μL stock culture of *A. catenella* strain Ac-LOHABE01 in the exponential phase. The parasitoids were propagated by sequentially transferring either aliquots of infected *A. catenella* cells or sporangia to exponentially growing *A. catenella* culture using the plant culture dish (SPL lifesciences, Gyeonggido, Korea). Each isolate is being maintained under the same growth conditions as the hosts described above. The dinoflagellate *A. catenella* was used as a host in all experiments during this study, otherwise stated.

Light microscopy: For light microscopic observations of life-cycle development and morphology of the different stages of the new parasitoid, the host *A. catenella* culture in exponential growth was inoculated in a 6-well plate (Corning, New York, USA) with recently formed (<3 h) zoospores, which were harvested by gravity filtration through Isopore membrane filters (10 μm pore size; Millipore, Cork, Ireland) from the parasite stock culture (Jeon et al. 2018), and was incubated for 4 d under the same growth conditions described above. At the start of the experiment, and at 12, 24, 36, 48, 54, 72 and 90 h after inoculation, light microscopic images of live infected host cells and mature sporangia were taken using an AxioCam HRc (Carl Zeiss Inc., Hallbergmoos, Germany) photomicrographic system coupled to an Axio Imager A2 (Carl Zeiss Inc., Hallbergmoos, Germany) equipped with differential interference contrast optics and epifluorescence capability. For observations of nuclear development and division, 200 μL of culture was fixed with 2% glutaraldehyde (final concentration), stained with 5X SYBR Gold (final concentration) (Molecular Probes, Eugene, Oregon USA) for 1 h, and photographed using an epifluorescence microscopy with blue light excitation (Filter Set 09; excitation BP 450-490, beam splitter FT 510, emission LP 515). Videos were recorded at 400× magnification using an inverted microscope (Axio Vert.A1, Carl Zeiss Inc., Hallbergmoos, Germany) equipped with a full HD mini box camera (MediCAM-Z, Comart System, Korea) to observe the process of zoospore release from sporangium. For enumeration of the zoospores in each sporangium, single mature sporangia were put into a hemocytometer individually and allowed to germinate in humid conditions. After the completion of germination, zoospores were fixed with acidic Lugol's solution and counted under the inverted microscopy at 200× magnification. At this time, the diameter of every sporangium was also measured using an AxioCam HRc photomicrograpic system coupled to an Axio Imager A2. The biovolume of the sporangium was calculated assuming a spherical body without considering the volume of the germ tubes, which were empty space when zoospores were at maturity.

Scanning electron microscopy (SEM): Infected cultures, sporangia at each developmental stage, or zoospores were fixed in 15 mL conical tube (Corning Inc., Corning, NY) with 2% glutaraldehyde (final concentration) for 1 h at 4 °C. Fixed infected cultures, sporangia, or zoospores were then filtered using Isopore membrane filters (10 μm pore size for both infected cultures and sporangia, and 0.8 μm for zoospores; Millipore, Cork, Ireland), washed in distilled water for 1 h and dehydrated in a graded ethanol series (25%, 50%, 70%, 99%) for 12 min at each step, and then rinsed three times in absolute ethanol for each 12 min. Samples were critical point dried in liquid CO_2 using an HCP-2 (Hitachi, Tokyo, Japan). Filters were subsequently glued to SEM stubs with carbon tape, sputter-coated with platinum and examined with a Hitachi HR-SEM (model SU-70, Hitachi, Tokyo, Japan) scanning electron microscope operating at 15 kV.

Transmission electron microscopy (TEM): For TEM, *Pyrophacus steinii* strain Ps-LOHABE01 was used as a host, instead of *A. catenella*, in which the infections by the new parasitoid were relatively low, thus making it difficult to easily observe the infected cells. Aliquots of the parasitoid cultures at each developmental stage were fixed with 2.5% glutaraldehyde (final concentration) buffered with 0.1 M cacodylate buffer at pH 7.4 and then stored at 4 °C until processed. The fixed samples were treated with 1% OsO4 plus 1.5% potassium ferrocyanide in 0.1 M phosphatate buffer (pH 7.3) for 1 h at 4 °C in the dark and embedded in Epon 812 after dehydration in an ethanol and propylene oxide series. Polymerization was conducted using pure resin at 70 °C for 2 d. Ultrathin sections (70 nm) were obtained with an ultramicrotome (UltraCut-UCT, Leica, Austria at Korea Basic Science Institute), which were then collected on 150 mesh copper grids. After staining with 2% uranyl acetate (10 min) and lead citrate (5 min), the sections were examined by transmission electron microcopy at 120 kV (Technai G2 Spirit Twin, FEI, Hillsboro, OR, USA).

DNA extraction: The single sporangia from the parasitoid cultures were individually isolated using a drawn glass micropipette, washed six times with sterile filtered seawater, placed into a PCR tube, and stored at −80 °C for 1 h. PCR tubes were thawed at room temperature for 5 min, added to 20 μL of 10% Chelex 100 resin solution (100–200 mesh, sodium form; Bio-Rad Laboratories, Hercules, CA, USA), and heated at 95 °C for 1 h. The tubes were centrifuged at 8,000 rpm at 4 °C for 1 min, and then each DNA in the supernatant was transferred to the new PCR tubes and stored at −20 °C until processed. In addition, free-living zoospores from the parasitoid cultures were harvested using Isopore membrane filters (10 μm pore size; Millipore, Cork, Ireland), transferred to a new 1.5 mL tube (Axygen Scientific, Union City, CA, USA), and concentrated by centrifugation at 13,000 rpm at 4 °C for 1 min. The obtained pellets were extracted using the Genomic DNA Extraction Kit (Bioneer, Daejeon, Korea) and stored at −20 °C until processed.

PCR amplification and sequencing: Polymerase chain reaction (PCR) amplifications were performed with eukaryotic primers Euk328f and Euk329r (Moon-van der Staay et al. 2001), Euk516r (Díez et al. 2001), and Euk1209r (Giovannoni et al. 1988) for SSU rRNA gene, and primers D1R and 28-1483R (Daugbjerg et al. 2000; Scholin et al. 1994) for LSU rRNA gene. PCRs were conducted in 25 μL of reaction solution containing 5 μL of DNA as a template, 2.5 μL of 10× Taq reaction buffer (containing 25 mM MgCl2), 0.5 μL of dNTP mix (10 mM), 0.75 μL of each primer (10 pmole μL-1), and 0.125 μL of Taq DNA polymerase (5 U μL-1, DT16-R500; Solgent Co., Daejeon, Korea). The reactions were conducted using an automated thermocycler (C1000 TouchTM Thermal Cycler, Bio-RAD, CA, USA) with the following conditions: for the SSU rRNA gene, the initial denaturing step was at 95 °C for 2 min, then 35 cycles of 20 s at 95 °C, 1 min 40 s at 55 °C, and 1 min 50 s at 72 °C, followed by a final extension step of 5 min at 72 °C; for the LSU rRNA gene, the initial denaturing step was at 95 °C for 2 min, then 35 cycles of 20 s at 95 °C, 40 s at 52 °C, and 1 min 30 s at 72 °C, followed by a final extension step of 5 min at 72 °C. Three microliter of the amplified PCR products was electrophoresed for 25 min at 100 V in a EcoDyeTM (SolGent Co., Daejeon, Korea) stained 1% agarose gels and then visualized under UV illumination. Amplified PCR products were purified with a LaboPass™ PCR Purification Kit (COSMO Genetech, Seoul, Korea) and sequenced with primers (Euk328f, Euk329r, Euk516r, and Euk1209r for SSU rRNA genes and D1R and 28-1483R for LSU rRNA gene) using a BigDye® Terminator v3.1 Cycle Sequencing kit (Applied Biosystems, Foster City, CA, USA) and an Applied Biosystems 3730xl DNA Analyzer, according to manufacturer's protocols at COSMO Genetech, in Seoul, Korea. The amplicons were sequenced until double stranded coverage using primer sets was reached. The sequences were aligned using the ContigExpress (Vector NTI version 10.1, Invitrogen, NY, USA), and low quality regions were manually checked. The SSU rDNA sequences of *Tuberlatum coatsi* obtained from both individually single sporangium and pellet extract of zoospores were all the same. Thus, all molecular data were obtained using DNA from pellet extract of zoospores. All sequences were verified by comparison using BLASTN search in the NCBI database and deposited in GenBank (accession no. MK309361 for SSU rDNA; MK309360 for LSU rDNA).

Alignment and phylogenetic analyses: The obtained sequences were primarily aligned with related sequences from Genbank database using ClustalW 1.6 (Thompson et al. 1994) and were further refined manually using MacGDE 2.4 (Linton 2005). Ambiguously aligned positions were removed and final alignments of 1585 positions for the SSU region and 2672 positions for SSU + LSU region were selected. Phylogenetic trees were inferred using the maximum likelihood (ML) and Bayesian inference methods. Modeltest v.3.7 (Posada and Crandall 1998) was performed to select the most appropriate model of substitution for the Maximum Likelihood (ML) method in PAUP. ML analyses were performed using RAxML (Stamatakis 2006) with the rapid bootstrapping option and 2,000 replicates. The GTRGAMMA evolution model was selected from MODELTEST using RAxML. GTR + I + G (−ln L = 11567.0732) and GTR +I + G (−ln L = 12069.2461) models were selected for SSU and SSU + LSU, respectively. Bayesian analysis was performed with MrBayes 3.1.1 (Ronquist et al. 2012) running four simultaneous Monte Carlo Markov Chains for 2,000,000 generations and sampling every 100 generations, following a burn in of 2,000 generations.

Acknowledgements

We gratefully acknowledge Ahsong Kim for her assistance during this work. This work was supported by research grants funded by the National Research Foundation of Korea (NRF-2016R1A6A1A03012647 and 2018R1A2B6003464).

Appendix A. Supplementary Data

Supplementary data associated with this article can be found, in the online version, at https://doi.org/10.1016/j.protis.2018.12.003.

References

Azevedo C (1989) Fine structure of *Perkinsus atlanticus* n. sp. (Apicomplexa, Perkinsea) parasite of the clam *Ruditapes decussatus* from Portugal. J Parasitol **75**:627–635

Bachvaroff TR, Gornik SG, Concepcion GT, Waller RF, Mendez GS, Lippmeier JC, Delwiche CF (2014) Dinoflagellate phylogeny revisited: Using ribosomal proteins to resolve deep branching dinoflagellate clades. Mol Phylogen Evol **70**:314–322

Bråte J, Logares R, Berney C, Ree DK, Klaveness D, Jakobsen KS, Shalchian-Tabrizi K (2010) Freshwater Perkinsea and marine-freshwater colonizations revealed by pyrosequencing and phylogeny of environmental rDNA. ISME J **4**:1144

Brugerolle G (2002) *Cryptophagus subtilis*: a new parasite of cryptophytes affiliated with the Perkinsozoa lineage. Europ J Protistol **37**:379–390

Casas SM, Grau A, Reece KS, Apakupakul K, Azevedo C, Villalba A (2004) *Perkinsus mediterraneus* n. sp., a protistan parasite of the European flat oyster *Ostrea edulis* from the Balearic Islands, Mediterranean Sea. Dis Aquat Org **58**:231–244

Chambouvet A, Berney C, Romac S, Audic S, Maguire F, De Vargas C, Richards TA (2014) Diverse molecular signatures for ribosomally 'active' Perkinsea in marine sediments. BMC Microbiol **14**:110

Chambouvet A, Gower DJ, Jirků M, Yabsley MJ, Davis AK, Leonard G, Maguire F, Doherty-Bone TM, Bittencourt-Silva GB, Wilkinson M (2015) Cryptic infection of a broad taxonomic and geographic diversity of tadpoles by Perkinsea protists. Proc Natl Acad Sci USA **112**:E4743–E4751

Daugbjerg N, Hansen G, Larsen J, Moestrup Ø (2000) Phylogeny of some of the major genera of dinoflagellates based on ultrastructure and partial LSU rDNA sequence data, including the erection of three new genera of unarmoured dinoflagellates. Phycologia **39**:302–317

Díez B, Pedrós-Alió C, Marsh TL, Massana R (2001) Application of denaturing gradient gel electrophoresis (DGGE) to study the diversity of marine picoeukaryotic assemblages and com-

parison of DGGE with other molecular techniques. Appl Environ Microbiol **67**:2942–2951

Figueroa RI, Garcés E, Massana R, Camp J (2008) Description, host-specificity, and strain selectivity of the dinoflagellate parasite *Parvilucifera sinerae* sp. nov. (Perkinsozoa). Protist **159**:563–578

Garcés E, Hoppenrath M (2010) Ultrastructure of the intracellular parasite Parvilucifera sinerae (Alveolata, Myzozoa) infecting the marine toxic planktonic dinoflagellate *Alexandrium minutum* (Dinophyceae). Harmful Algae **10**:64–70

Giovannoni SJ, DeLong EF, Olsen GJ, Pace NR (1988) Phylogenetic group-specific oligodeoxynucleotide probes for identification of single microbial cells. J Bacteriol **170**:720–726

Hoppenrath M, Leander BS (2009) Molecular phylogeny of *Parvilucifera prorocentri* (Alveolata, Myzozoa): Insights into perkinsid character evolution. J Eukaryot Microbiol **56**:251–256

Jeon BS, Nam SW, Kim S, Park MG (2018) Revisiting the *Parvilucifera infectans*/*P. sinerae* (Alveolata Perkinsozoa) species complex, two parasitoids of dinoflagellates. Algae **33**:1–19

Leander BS, Hoppenrath M (2008) Ultrastructure of a novel tube-forming, intracellular parasite of dinoflagellates: *Parvilucifera prorocentri* sp. nov. (Alveolata, Myzozoa). Europ J Protistol **44**:55–70

Lepelletier F, Karpov SA, Le Panse S, Bigeard E, Skovgaard A, Jeanthon C, Guillou L (2014) *Parvilucifera rostrata* sp. nov. (Perkinsozoa), a novel parasitoid that infects planktonic dinoflagellates. Protist **165**:31–49

Lepère C, Domaizon I, Debroas D (2008) Unexpected importance of potential parasites in the composition of the freshwater small-eukaryote community. Appl Environ Microbiol **74**:2940–2949

Levine ND (1978) Perkinsus gen. n. and other new taxa in the protozoan phylum Apicomplexa. J Parasitol **64**:549

Linton E (2005) MacGDE: genetic data environment for MacOS X, Software available at http://www. msu.edu/?lintone/macgde

Mangot J-F, Debroas D, Domaizon I (2011) Perkinsozoa, a well-known marine protozoan flagellate parasite group, newly identified in lacustrine systems: a review. Hydrobiologia **659**:37–48

McLaughlin S, Tall B, Shaheen A, Elsayed E, Faisal M (2000) Zoosporulation of a new Perkinsus species isolated from the gills of the softshell clam Mya arenaria. Parasite **7**:115–122

Moon-van der Staay SY, De Wachter R, Vaulot D (2001) Oceanic 18S rDNA sequences from picoplankton reveal unsuspected eukaryotic diversity. Nature **409**:607–610

Norén F, Moestrup Ø, Rehnstam-Holm A-S (1999) *Parvilucifera infectans* Norén et Moestrup gen. et sp. nov. (Perkinsozoa phylum nov.): a parasitic flagellate capable of killing toxic microalgae. Europ J Protistol **35**:233–254

Posada D, Crandall KA (1998) Modeltest: testing the model of DNA substitution. Bioinformatics (Oxford, England) **14**:817–818

Reñé A, Alacid E, Ferrera I, Garcés E (2017a) Evolutionary trends of Perkinsozoa (Alveolata) characters based on observations of two new genera of parasitoids of dinoflagellates, *Dinovorax* gen. nov. and *Snorkelia* gen. nov. Front Microbiol **8**:1594

Reñé A, Alacid E, Figueroa RI, Rodríguez F, Garcés E (2017b) Life-cycle, ultrastructure, and phylogeny of Parvilucifera corolla sp. nov.(Alveolata, Perkinsozoa), a parasitoid of dinoflagellates. Europ J Protistol **58**:9–25

Ronquist F, Teslenko M, Van Der Mark P, Ayres DL, Darling A, Höhna S, Larget B, Liu L, Suchard MA, Huelsenbeck JP (2012) MrBayes 3. 2: efficient Bayesian phylogenetic inference and model choice across a large model space. Syst Biol **61**:539–542

Scholin CA, Herzog M, Sogin M, Anderson DM (1994) Identification of group-and strain-specific genetic markers for globally distributed Alexandrium (Dinophyceae). II. Sequence analysis of a fragment of the LSU rRNA gene. J Phycol **30**:999–1011

Stamatakis A (2006) RAxML-VI-HPC: maximum likelihood-based phylogenetic analyses with thousands of taxa and mixed models. Bioinformatics **22**:2688–2690

Thompson JD, Higgins DG, Gibson TJ (1994) CLUSTAL W: improving the sensitivity of progressive multiple sequence alignment through sequence weighting, position-specific gap penalties and weight matrix choice. Nucleic Acids Res **22**:4673–4680